

## Delayed evolutionary branching in small populations

David Claessen,<sup>1\*</sup> Jens Andersson,<sup>2‡</sup> Lennart Persson<sup>2</sup>  
and André M. de Roos<sup>1</sup>

<sup>1</sup>*Institute for Biodiversity and Ecosystem Dynamics, University of Amsterdam, PO Box 94084, 1090 GB Amsterdam, The Netherlands and* <sup>2</sup>*Department of Ecology and Environmental Science, Umeå University, SE-90187 Umeå, Sweden*

---

### ABSTRACT

**Question:** How is the process of evolutionary branching influenced by demographic stochasticity?

**Mathematical methods:** Adaptive dynamics of (i) a simple consumer-resource model and (ii) an analogous but individual-based model with finite population size.

**Key assumptions:** Consumers have access to two habitats with dynamic resources. The fraction of time spent in each habitat is the evolving trait. System size influences absolute population size and hence demographic stochasticity but not the expected population densities. Reproduction is asexual.

**Predictions:** Absolute population size is an ecological factor that controls the outcome of evolutionary dynamics by modifying the level of demographic stochasticity. Small populations are predicted to remain monomorphic generalists while large populations are predicted to split evolutionarily into specialized sub-populations. Underlying the delayed or absent evolutionary branching in small populations are (i) random genetic drift and (ii) extinction of incipient branches due to near-neutral stability.

*Keywords:* adaptive dynamics, demographic stochasticity, evolutionary branching, extinction, finite population size, incipient species, random genetic drift.

### INTRODUCTION

‘Adaptive dynamics’ is a theoretical framework for studying evolutionary dynamics in an ecological context. This theory asserts that evolution takes place in a dynamic fitness landscape in which fitness is the outcome of ecological interactions between individuals such as competition for food or for mates (Metz *et al.*, 1992). Central to the theory are the classification of evolutionary scenarios based on the geometry of the invasion-fitness function (Metz *et al.*, 1996; Geritz *et al.*, 1998) and the so-called canonical equation of adaptive dynamics, which predicts the rate and direction of evolution (Dieckmann and Law, 1996; Champagnat *et al.*, 2001).

---

\* Author to whom all correspondence should be addressed. e-mail: david.claessen@ens.fr

‡ Present address: County Administrative Board of Jämtlands Län, SE-83186 Östersund, Sweden.

Consult the copyright statement on the inside front cover for non-commercial copying policies.

---

A great deal of the theory, including the above-mentioned classification and canonical equation, is based on simplifying assumptions that allow for the derivation of analytical results (Metz *et al.*, 1996). Two of these assumptions – i.e. that (i) mutations are rare and (ii) mutations have small phenotypic effect – have recently been discussed extensively in the literature (Van Dooren, 2005; Waxman and Gavrilets, 2005a, 2005b, and references therein). Here we focus on another common assumption, which is that (iii) the current population is large enough that demographic stochasticity and random genetic drift in the resident population can be ignored. Although demographic stochasticity in the mutant populations is implicitly incorporated in the canonical equation, it is ignored for the resident population. Demographic stochasticity results from discrete random events such as birth and death. In very large populations, these events have tiny effects and occur frequently enough to result in predictable and almost smooth changes of population density. The population dynamics are then well-approximated by a deterministic model. In small populations, however, the discrete events occur less frequently and moreover each event has a greater influence on the state of the population. In this case the population size and genetic composition may deviate significantly from the expectation based on a deterministic model. Natural populations are of finite size and hence subject to demographic stochasticity, and therefore the sensitivity of theoretical predictions to relaxing assumption (iii) is of great importance, especially in the context of confronting model predictions with empirical data on ecological systems. Note that natural populations are also subject to environmental stochasticity; this, however, is outside the scope of this paper.

Analytical predictions of adaptive dynamics have often been tested with individual-based simulation models in which population numbers are finite (and in which assumptions (i–iii) may be relaxed) (e.g. Dieckmann and Doebeli, 1999; van Doorn *et al.*, 2004). The analytical predictions are usually found to hold in such simulations but a full understanding of the effect of absolute population size is still lacking.

One line of studies on evolutionary dynamics in finite populations is game-theoretic and investigates the consequences of the fact that a single mutant cannot play against itself (Riley, 1979; Schaffer, 1988). The evolutionarily stable strategy (ESS) then appears to depend on absolute population size: the smaller the population, the more spiteful the ESS (Schaffer, 1988). A second line of research addresses the effect of demographic stochasticity on evolutionary dynamics. Proulx and Day (2001) argue that the expected growth rate of a small mutant population [the standard definition of fitness in adaptive dynamics theory (Metz *et al.*, 1992)] may not accurately predict the direction and endpoint of evolution in finite populations subject to environmental stochasticity. In the absence of demographic stochasticity, alleles with a negative expected growth rate have zero probability to reach fixation. Proulx and Day (2001) show that in a finite population they may yet have a fixation probability that is greater than that of a neutral allele. They argue that it is hence more correct to use the fixation probability of rare alleles to describe the evolutionary dynamics of small populations. Cadet *et al.* (2003) and Parvinen *et al.* (2003) study the evolution of the dispersal rate in a metapopulation model and demonstrate that accounting for finite population size in local patches alters the evolutionary prediction. They propose two explanations for the difference. First, when local populations are small, the relatedness of individuals is high, leading to kin competition. Second, demographic stochasticity results in variation in local population size such that a disperser from a non-empty patch always has a chance to find a patch with fewer competitors. Both explanations favour the evolution of a higher dispersal rate under the influence of demographic stochasticity. In conclusion, these studies show that

the direction of evolution in finite populations may differ from the expectation based on a deterministic model.

An important finding of adaptive dynamics theory is that ‘upward’ movement in a dynamic fitness landscape (i.e. resulting from directional selection) can take an evolving population towards a fitness minimum referred to as an ‘evolutionary branching point’ (Metz *et al.*, 1992). At this point, selection turns disruptive and (depending on the mating system) the population may branch into two sympatrically diverging subpopulations (Metz *et al.*, 1992; Dieckmann and Doebeli, 1999) or a genetic polymorphism (Kisdi and Geritz, 1999). In this paper, we focus specifically on the effect of finite population size on the dynamics of evolutionary branching. We ask the question: ‘How is the process of evolutionary branching influenced by demographic stochasticity?’ The answer to the question may be used to confront theoretical predictions with a comparative study of empirical data on a range of population sizes.

As the starting point for our study, we choose a very simple model for which evolutionary branching is predicted according to current adaptive dynamics theory. Several modelling studies have demonstrated that a consumer population exploiting two distinct food populations or habitats can evolve to an evolutionary branching point and hence potentially speciate or give rise to a genetic polymorphism (e.g. Kisdi and Geritz, 1999; Day, 2000; Claessen and Dieckmann, 2002; Schreiber and Tobiasen, 2003; Rueffler *et al.*, 2004, 2006). Generally, the condition for evolutionary branching in such models is that the generalist strategy exploiting both resources has a lower fitness than mutant strategies with a slightly higher degree of specialization in either direction. In other words, the shape of the trade-off between the performance (contribution to fitness) in the two habitats determines the outcome of the evolutionary dynamics. When fitness is a linear combination of performance in two habitats (as is the case here), evolutionary branching is expected if the trade-off is ‘strong’ (convex), whereas an evolutionarily stable generalist is expected if the trade-off is ‘weak’ (concave) or ‘neutral’ (linear) (Rueffler *et al.*, 2004, 2006).

We model a consumer population feeding on two resource populations that are assumed to occur in different habitats. The evolutionary trait is assumed to be the fraction of time spent in each habitat. If the functional response in each habitat does not depend directly on the trait value (but only indirectly through the effect on prey density), such time splitting amounts to a linear trade-off. The reason is that individuals cannot be in two habitats at the same time. However, if the functional response is a function of the trait value, the trade-off becomes non-linear. We assume that the habitat-specific foraging capacity increases with the time spent in the habitat. The foraging performance of individuals in a given habitat may improve with time by, for example, phenotypic plasticity or learning. Our deterministic model is very similar to that of Schreiber and Tobiasen (2003), who model the effects of different resource relations (essential, substitutable, antagonistic) and find that antagonistic resources may induce evolutionary branching. In our model, however, the resources are always substitutable and branching is caused by the trade-off in attack rates.

Our model is loosely based on the ecology of lake fish such as Arctic charr (*Salvelinus alpinus*), perch (*Perca fluviatilis*), and sticklebacks (*Gasterosteus aculeatus*). Such species often have access to two resources in different habitats: zooplankton in the pelagic habitat and macroinvertebrates in the benthic habitat. For a number of fish species, it has been demonstrated that diet influences individual development and morphology, resulting in increased habitat-specific foraging capacity (Robinson and Wilson, 1995; Day and McPhail, 1996; Andersson, 2003; Andersson *et al.*, 2005). A strong trade-off results if the resources occur in different habitats

and habitat-specific foraging ability is positively related to the amount of time spent in the habitat.

We use an individual-based model to show that absolute population size influences the probability of successful evolutionary branching. In our model, lake volume scales the total population size without affecting the ecological interactions. The only difference between small and large systems is thus the level of demographic stochasticity. By studying the evolutionary dynamics for different lake sizes, we gain insight into the effect of this stochasticity on evolutionary branching.

Since we are specifically interested in the effect of stochasticity on evolutionary branching, we choose to keep the model as simple as possible. The species that inspired this study (Arctic charr) is a sexual species whose populations are size structured (J. Andersson *et al.*, submitted). However, in this paper we choose to ignore both these aspects in order to focus exclusively on the effect of absolute population size.

## THE MODEL

### Deterministic model

We model an unstructured, asexual consumer population whose density is denoted by  $N(t)$  and two resource populations whose densities are denoted by  $F_1(t)$  and  $F_2(t)$  and which are assumed to occur in two different habitats. We assume that the consumers have a heritable trait denoted by  $u$ , which is the fraction of their lifetime they spend foraging on resource 1, while they spend the remaining fraction  $(1 - u)$  foraging on the other resource. Note that  $u$  is hence restricted to the interval  $(0, 1)$ . For simplicity, we assume a Holling type 1 functional response, i.e. linear in prey density (but we have checked a model with a type 2 functional response that gave qualitatively the same results). We assume that the per capita birth rate is proportional to the consumption rate:

$$\beta(u) = k_1 F_1(t) A_1(u) u + k_2 F_2(t) A_2(u) (1 - u) \quad (1)$$

where  $k_1$  and  $k_2$  are the efficiencies of converting food into offspring.  $A_1(u)$  and  $A_2(u)$  are the search rates in the two habitats (or ‘attack rates’; volume cleared of prey per unit of time). They are functions of  $u$  because we assume that the foraging ability on a resource depends on the time spent foraging on that resource. As a phenomenological model, we assume simple linear relations between  $u$  and the search rates:

$$A_1(u) = a_1 + b_1 u \quad (2)$$

$$A_2(u) = a_2 + b_2 u \quad (3)$$

The assumption that foraging capacity depends on the time spent foraging is based on experimental measurements in freshwater fish species (Andersson, 2003; Andersson *et al.*, 2005). For Arctic charr, it has been demonstrated that exposure of juveniles during ontogeny to zooplankton prey, macroinvertebrate prey or a mixture of both influences the foraging performance at the end of the experiment [associated with a morphological effect (Andersson, 2003)]. A zooplankton diet increases the search rate on zooplankton, but diet has no effect on the search rate for macroinvertebrates. In terms of equations (2) and (3), this is modelled as  $b_1 > 0$  and  $b_2 = 0$  (assuming that habitat 1 is the pelagic habitat). We assume  $b_1 = 1$ ,  $b_2 = 0$ ,  $a_1 = 1$ , and  $a_2 = 1.5$ , resulting in an asymmetric, strong trade-off (Fig. 1e,f).

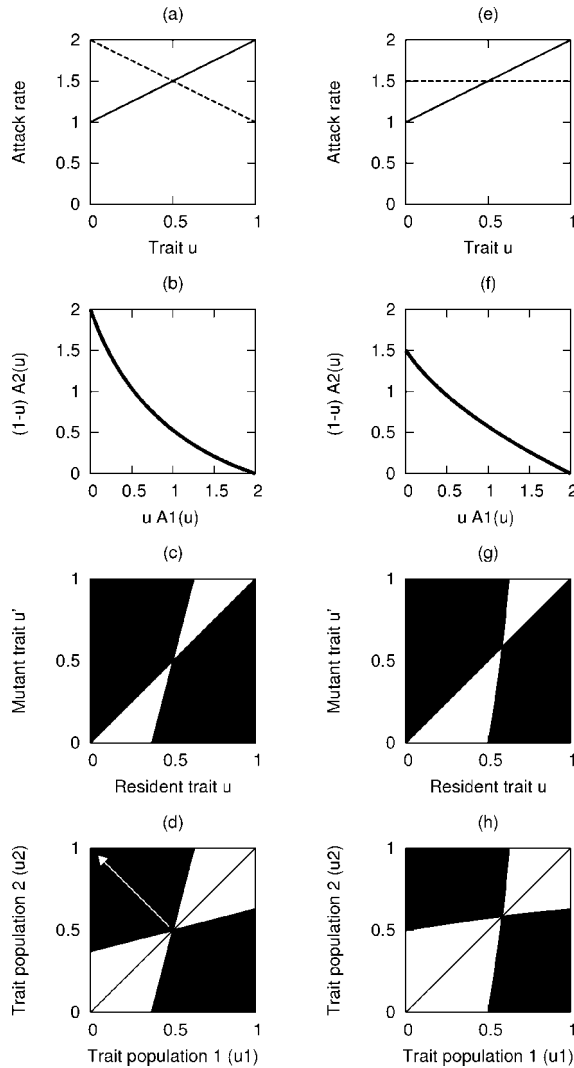


**Fig. 1.** (a–d) The symmetric trade-off  $a_1 = 1, a_2 = 2, b_1 = 1, b_2 = -1$ . (a) The search rate (equations 2–3) in habitat 1 (solid) and habitat 2 (dashed) vs. time spent in habitat 1. (b) The per-capita search effort in habitat 2 versus the one in habitat 1 reveals a strong (i.e. convex) trade-off. (c) The pairwise-invasibility plot (PIP). Shown is the invasion fitness (black: positive; white: negative) of a mutant with trait  $u'$  given the resident has trait  $u$  and is at ecological equilibrium. The point  $u^* = 0.5$  is an evolutionary branching point (EBP). (d) The trait evolution plot (TEP). The black area is the co-existence area defined as the set of pairs of traits which can mutually invade each other (set of protected polymorphisms). The arrow indicates the expected trajectory of  $u_1$  and  $u_2$ . (e–h) The same as (a–d) but for Arctic charr parameters  $a_1 = 1, a_2 = 1.5, b_1 = 1, b_2 = 0$ . The point  $u^* = 0.58$  is an EBP. Other parameters:  $K_1 = K_2 = 1, \delta_1 = \delta_2 = 1, \mu = 0.1$ .

The total per capita search effort in a habitat equals the time that an individual spends in that habitat, multiplied with the search rate:  $x_1(u) = uA_1(u)$  for habitat 1 and  $x_2(u) = (1 - u)A_2(u)$  for habitat 2. A strong trade-off between search effort in the two

habitats is obtained if  $b_1/(a_1 + b_1) > b_2/a_2$ , and a weak trade-off with the opposite inequality. Plotting  $x_1(u)$  versus  $x_2(u)$  shows the shape of the trade-off. Figure 1a shows an example where the search rates in both habitats increase with time spent in that habitat ( $b_1 = 1$ ,  $b_2 = -1$ ,  $a_1 = 1$ , and  $a_2 = 2$ ). Figure 1b shows the resulting strong trade-off in the plot of  $x_1(u)$  versus  $x_2(u)$ . Figure 1e shows a parameterization of the search rates based on the observations in Arctic charr, which also leads to a strong trade-off (Fig. 1f).

The resources are assumed to have no direct interaction with each other, and to follow semi-chemostat dynamics, which has been argued to appropriately describe resource dynamics in systems of size-selective fish foraging on zooplankton (Persson *et al.*, 1998). Assuming a consumer population monomorphic in trait  $u$ , the deterministic dynamics of the three populations are described by the following set of ordinary differential equations (ODEs):

$$\frac{dN}{dt} = (\beta(u) - \mu)N(t) \quad (4)$$

$$\frac{dF_1}{dt} = \delta_1(K_1 - F_1(t)) - F_1(t)N(t)A_1(u)u \quad (5)$$

$$\frac{dF_2}{dt} = \delta_2(K_2 - F_2(t)) - F_2(t)N(t)A_2(u)(1 - u) \quad (6)$$

where  $\mu$  is a constant mortality rate,  $\beta(u)$  is the per capita birth rate as defined in equation (1), and  $\delta_1$  and  $\delta_2$  are the renewal rates of the two resource populations. This deterministic formulation is appropriate for very large systems only; the model for populations in smaller lakes needs to incorporate demographic stochasticity and is described in the next sub-section.

### Stochastic model

In finite populations, the number of consumer individuals is an integer number denoted by  $n(t)$ . The consumer density  $N(t)$  is found by dividing by the lake volume  $V$ , thus  $N(t) = n(t)/V$ . Very large systems (i.e.  $V \rightarrow \infty$ ) have so many individuals that discrete events at the level of individuals (i.e. births and deaths) each have very small effects. The changes in the population density  $N(t)$  are then well-approximated by the deterministic model (equations 4–6). For small systems, however, these discrete events cannot be ignored. The deterministic (mean field) model can still be used to estimate the long-term average densities  $\tilde{N}$ ,  $\tilde{F}_1$ , and  $\tilde{F}_2$  by the equilibrium of equations (4–6), but the actual values will deviate from these values due to demographic stochasticity.

Each of the  $n(t)$  consumer individuals is characterized by its trait value  $u_i$  (where  $i = 1, \dots, n(t)$ ), which determines its use of the resources as described in the ODE model. The number of individuals changes through discrete birth and death events. The rate at which birth and death events occur depends on the number of individuals, their individual birth rates  $\beta(u_i)$ , and the death rate  $\mu$ . We describe the dynamics of a finite population using an individual-based, discrete event simulation model (i.e. a birth–death process in continuous time). Details of the simulation procedure are given in the Appendix.

In this paper, we assume clonal reproduction (sexual reproduction is discussed elsewhere). Offspring have the same genotype  $u$  as their parent unless, with probability  $P$ , a mutation

occurs. In the case of a mutation, the newborn's trait value is drawn from a truncated normal distribution with standard deviation  $\sigma$  around the trait value of its clonal parent. If the drawn value is below 0 or above 1, it is replaced by 0 or 1, respectively.

Compared with the consumer population, the resources (zooplankton and macro-invertebrates) are much more numerous, with smaller body sizes and shorter generation times. Therefore, we choose to model their dynamics with ODEs analogously to equations (5–6) (see Appendix).

In the absence of mutations ( $P = 0$ ), the individual-based model (IBM) defined like this is completely analogous to the deterministic model. In the limit of a very large lake volume ( $V \rightarrow \infty$ ), the dynamics of  $n(t)/V$  and the resource densities converge to equations (4–6).

## RESULTS

### Population dynamics

#### *Deterministic*

First, we scale away the conversion efficiencies by choosing scaled prey densities  $F'_1 = F_1/k_1$  and  $F'_2 = F_2/k_2$ . Below, we assume parameter values that allow a monomorphic consumer population to have a positive population density in the entire interval of  $u \in (0, 1)$ . In terms of the model parameters, this requires that  $\delta_1$ ,  $\delta_2$ ,  $K_1$ , and  $K_2$  are positive and

$$0 < \mu < k_1 K_1 (a_1 + b_1 u) u + k_2 K_2 (a_2 + b_2 u) (1 - u)$$

for all  $u$ . We also require that  $a_1$  and  $a_2$  are positive and  $b_1 > -a_1$  and  $b_2 > -a_2$  such that the functions  $A_1(u)$  and  $A_2(u)$  have positive values for all  $u$ .

For the limiting cases  $u = 0$  and  $u = 1$ , it can be shown analytically that the equilibrium of equations (4–6) is always stable (results not shown). An analytical result for the stability of the equilibrium for  $0 < u < 1$  could not be obtained. Instead, the dynamics of equations (4–6) were studied using the software Content for numerical bifurcation analysis (Kuznetsov, 1995). We studied the stability of the internal equilibrium (i.e. positive densities of all three populations) for large ranges of all parameters. The dynamics were always found to converge to a stable equilibrium point ( $\tilde{N}$ ,  $\tilde{F}_1$ ,  $\tilde{F}_2$ ) (results not shown). Population cycles or alternative stable states were not found. Note that a linear functional response and semi-chemostat resource growth tend to produce more stable dynamics than a saturating functional response and/or logistic growth.

#### *Stochastic*

The dynamics of the individual-based model were studied with simulations. All else being equal, the variability around the expected steady state increases if the lake volume  $V$  decreases: according to the scaling rule for demographic stochasticity (Desharnais *et al.*, 2006), the coefficient of variation of population size is expected to scale like  $\text{CV}(n) \propto n^{-0.5}$  (or, equivalently,  $\text{CV}(n) \propto V^{-0.5}$ ). To establish a relation between the coefficient of variation (CV) of population abundance and lake volume, we used simulations without mutations ( $P = 0$ ) and with a generalist consumer strategy ( $u = 0.5$ ), for  $10^4$  time units and for a range of lake volumes between  $V = 1$  and  $V = 1000$ . For each lake volume, we computed the CV of abundance as  $\text{SD}(n(t))/\tilde{n}$ , where  $\tilde{n}$  denotes the average abundance and SD denotes the standard deviation. A power function  $\text{CV} = c_1 V^{c_2}$  was fitted to the measured

coefficient of variation of population abundance  $n(t)$ . Simulations of the IBM with  $u = 0.5$  and  $P = 0$  show that the coefficient of variation of abundance scales like

$$\text{CV}(n) \approx 0.3(V)^{-0.5} = 1.3(\tilde{n})^{-0.5}$$

For the parameter values used in Fig. 2 and with  $u = 0.5$ , the expected number of consumers equals  $\tilde{N} = 18.7 V$ , while for  $\hat{u} = 0$  it is  $\tilde{N} = 9.5 V$ . Demographic extinction occurs frequently when lake volume drops below  $V = 2$ , yet all runs with  $V = 2$  persisted for more than  $10^5$  generations and all runs with  $V = 3$  for at least  $10^7$  generations.

### Adaptive dynamics in large systems

In large lakes, the adaptive dynamics of our stochastic model are straightforward (Fig. 2a). In the initial phase of the evolutionary dynamics, the resident population is monomorphic with  $u \approx 0$ . Habitat 1 is more or less unexploited and hence close to its carrying capacity, while habitat 2 is depleted. Directional selection then leads to the invasion of mutants that spend more time in habitat 1 and less time in habitat 2. This can be seen from the pairwise-invasibility plot (PIP) (van Tienderen and de Jong, 1986): if the resident has a low trait value,

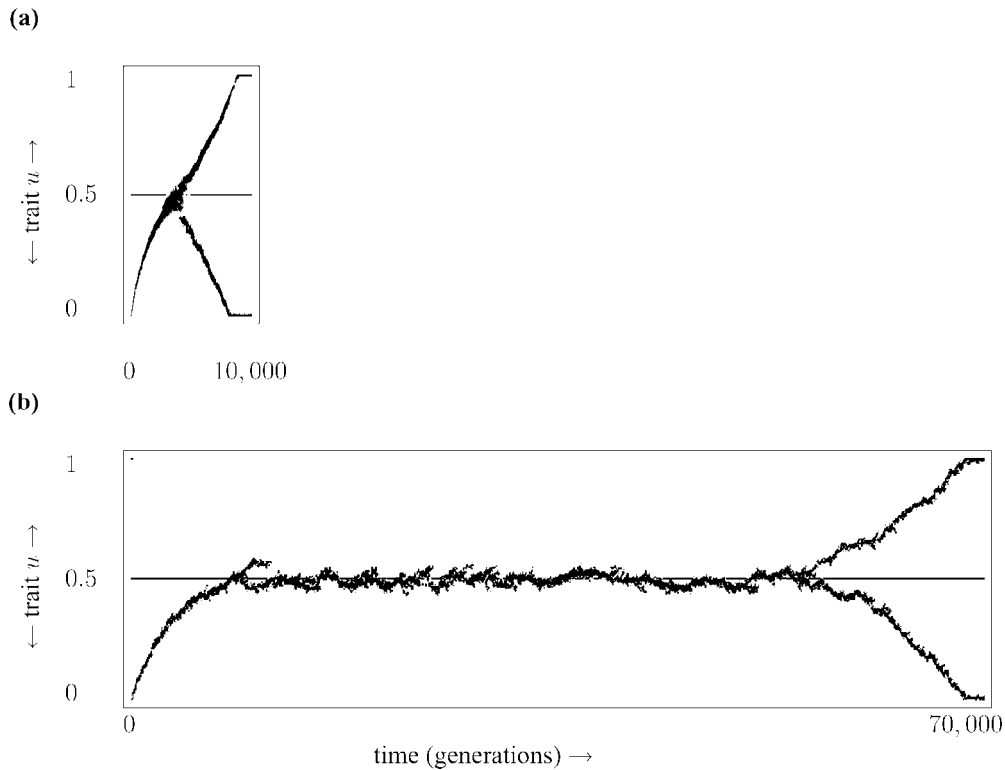


**Fig. 2.** Examples of adaptive dynamics in a big lake (a,  $V = 1000$ ) and a small lake (b,  $V = 40$ ), assuming a symmetric trade-off (Fig. 1a–d). Depicted is the trait distribution  $n(u)$  at time  $t$ . Maximum divergence ( $\Delta u = 1$ ) is reached after  $t = 8600$  and  $t = 69,000$  generations, respectively. Time axes in (a) and (b) have the same scale. Other parameters:  $K_1 = K_2 = 1$ ,  $\delta_1 = \delta_2 = 1$ ,  $\mu = 0.1$ ,  $P = 0.1$ ,  $\sigma = 0.002$ .

then only mutants with a higher trait value ( $u' > u$ ) have positive invasion fitness (Fig. 1c). As the average trait value  $\hat{u}$  gradually increases, the population feedback results in a balancing of the two resources: habitat 1 becomes more exploited while habitat 2 is released, reducing the selection gradient. The two habitats are ‘balanced’ when the consumption rate from the two habitats is equal:  $F_1(t)A_1(\hat{u})\hat{u} = F_2(t)A_2(\hat{u})(1 - \hat{u})$ , at which point the directional selection vanishes. The resident trait value that balances the resources is the evolutionary attractor of the monomorphic dynamics and is denoted by  $u^*$ . The value of  $u^*$  depends on the parameter values:  $u^* = 0.5$  with the symmetric trade-off (Fig. 1c) and  $u^* = 0.58$  with the trade-off based on Arctic charr (Fig. 1g), assuming  $K_1 = K_2 = 1$  and  $\mu = 0.1$ .

When the resources are balanced, evolution is no longer driven by resource densities but by the constraints imposed by the trade-off. In the case of a strong trade-off, the resident with trait  $\hat{u} = u^*$  is located at a fitness minimum: mutations in both directions have positive invasion fitness (Fig. 1c). Consequently, selection becomes disruptive when  $\hat{u}$  approaches  $u^*$  and the asexual population can split into two sub-populations (Fig. 2a). A trait value that is both convergent stable (in the monomorphic dynamics) and evolutionarily unstable is referred to as an evolutionary branching point (EBP hereafter) (Geritz *et al.*, 1998). By contrast, in the case of a weak trade-off, selection becomes stabilizing at this point and the population remains monomorphic with trait  $\hat{u} = u^*$  (not shown).

After the split of the population into two incipient species, a rough demarcation of the course of the co-evolution of the two populations can be derived from a graph referred to as the ‘trait evolution plot’ or TEP (Geritz *et al.*, 1998). This plot is constructed in three steps. The first step is to mark the areas for which a population with trait  $u_2$  can invade the monomorphic equilibrium of a population with trait  $u_1$  (i.e. the PIP). The second step is to mark the areas for which  $u_1$  can invade  $u_2$  (i.e. the PIP mirrored in the diagonal  $y = x$ ). The areas that were marked twice (black areas in Fig. 1d) correspond to combinations of  $u_1$  and  $u_2$  which are mutually invulnerable and is referred to as the co-existence area or the set of protected polymorphisms (Metz *et al.*, 1996). The third step is to mark, in the co-existence area, the points at which the fitness gradient is zero for one of the two branches, i.e. isoclines of the co-evolutionary dynamics. In the current model, the TEP has no isoclines; rather, the TEP predicts divergent co-evolutionary dynamics to  $(\hat{u}_1, \hat{u}_2) = (0, 1)$  if  $u^*$  is an EBP (Fig. 1d).

Co-existence of two emerging branches is likely only if their mean strategies, referred to as  $\hat{u}_1$  and  $\hat{u}_2$ , are within the co-existence area. When a pair of traits of the incipient species  $(u_1, u_2)$  moves out of the co-existence area (for some reason), one of the two branches is forced to extinction (i.e. its expected population size becomes zero), while the other one settles at its monomorphic equilibrium density (Metz *et al.*, 1996). In Fig. 2a, branching is followed by symmetrical divergence of  $\hat{u}_1$  and  $\hat{u}_2$ . Projected onto the TEP the trajectory of  $(\hat{u}_1, \hat{u}_2)$  is expected to be well inside the co-existence area, close to a straight line from the evolutionary branching point  $(u^*, u^*)$  to the final point  $(0, 1)$  (Fig. 1d), but will deviate from it because mutations make random and finite steps.

### The effect of lake size on evolutionary branching

The effect of lake volume on the adaptive dynamics in the IBM model is clearly illustrated with two examples in Fig. 2 showing the dynamics of the trait distribution in simulations of two lakes of different volume ( $V = 1000$  and  $V = 40$  units, respectively, corresponding to

$\tilde{n} = 18,700$  and  $\tilde{n} = 748$  for  $u = 0.5$ ). Both runs start with ten individuals with a trait value of  $u = 0$ . Note that the only ecological difference between the two lakes is their volumes. Hence given the same monomorphic trait value, the expected time-averaged densities ( $\tilde{N}$ ,  $\tilde{F}_1$ ,  $\tilde{F}_2$ ) are the same in the two lakes. The two examples demonstrate three ways by which the evolutionary dynamics differ in the two lakes. First, in the small lake evolutionary change is slower; it takes longer both to approach the evolutionary attractor  $u^*$  and to diverge after branching. Second, in the small lake evolutionary branching is frequently followed by extinction of one of the incipient branches. Third, in the small lake the trait distribution fluctuates around  $u^*$ , such that the mean trait in the population,  $\hat{u}$ , spends little time at  $u^*$ . The waiting time to eventual branching is much larger in the small lake, mainly for the two latter reasons.

These three observations are quantified more thoroughly in Fig. 3, which summarizes results for a range of lake volumes between  $V = 1$  and  $V = 1000$ . For each lake volume ten simulations of the individual-based model were run, starting with ten individuals with a trait value of  $u = 0$ . Simulations ran for a maximum of  $10^8$  time units or shorter if branching occurred before that time.

Figure 3a shows the approach time, denoted by  $t_A$  and defined as the period until the mean trait  $\hat{u}(t)$  has approached the evolutionary attractor  $u^*$  to within 5%. The approach time  $t_A$  decreases gradually with increasing lake volume because mutants appear more frequently in large populations than in small ones. Figure 3b shows the ‘branching delay’, denoted by  $\Delta_B$ , defined as the time elapsed between approaching the attractor and the moment of branching:  $\Delta_B = t_B - t_A$ , where  $t_B$  is the time at branching. To detect branching, we subdivide the trait distribution into a lower, middle, and upper class. The middle class is defined as the central 10% of the current range of  $u$  in the population. Branching is defined as a moment when the middle class becomes empty. If during a single run multiple branching events occur (due to extinction of incipient branches), then  $t_B$  is defined as the last one. A striking result is that the branching delay ( $\Delta_B$ ) increases dramatically when lake volumes drop below  $V = 100$ ; in lakes with a volume below  $V = 20$ , branching is not observed within  $10^8$  time units ( $10^7$  generations). The cause of this result will be discussed below. Figure 3c shows the divergence delay, denoted by  $\Delta_D$  and defined as  $\Delta_D = t_D - t_B$ , where  $t_D$  is the first moment that the population contains individuals with  $u = 0$  and  $u = 1$  at the same time. The divergence delay  $\Delta_D$  decreases slowly with lake volume, again because mutants appear more frequently in large populations than in small ones.

#### *Sensitivity to mutation rate and step size*

Quantitative aspects of the pattern in Fig. 3 depend on the width of the mutation distribution and hence on the mutation probability  $P$  and the standard deviation of the mutation steps  $\sigma$ . Figure 4 shows results for the Arctic charr parameters and four different combinations of  $P$  and  $\sigma$ . The figures show the same pattern of  $t_A$  and  $\Delta_B$  as discussed above (cf. Fig. 3a,b). Increasing  $\sigma$  or  $P$  has a large quantitative influence; it results in a reduction of both the smallest observed time to branching and the minimum lake volume in which branching can occur. The smallest observed branching delay in large lakes ranges from 100 generations ( $\sigma = 0.05$ ,  $P = 0.01$ ) to 5000 generations ( $\sigma = 0.01$ ,  $P = 10^{-4}$ ). These patterns are confirmed by the results with a symmetric trade-off over the entire range of  $P$  and  $\sigma$  (data not shown). Despite these quantitative differences, for all values of  $P$  and  $\sigma$  a qualitative result holds: there is a critical lake volume  $V_{\text{crit}}$  below which evolutionary branching is not expected to occur within an ecologically realistic time scale (if ever).

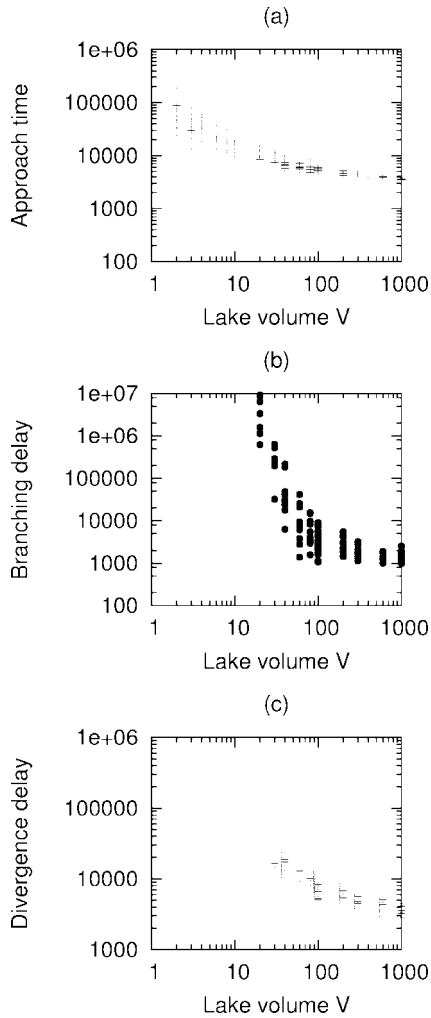


**Fig. 3.** The three phases of adaptive dynamics computed for ten simulations per lake volume, assuming a symmetric trade-off (Fig. 1a–d). Time is expressed in units of the average life span ( $1/\mu$ ). All runs with  $V=1$  are extinct before approaching the attractor. (a) Approach time  $t_A$ . (b) Branching delay  $\Delta_B$ . (c) Divergence delay  $\Delta_D$ . Parameters:  $K_1 = K_2 = 1$ ,  $\delta_1 = \delta_2 = 1$ ,  $\mu = 0.1$ ,  $P = 0.1$ ,  $\sigma = 0.002$ .

### Why is branching hard in small lakes?

Inspection of Fig. 2b suggests two processes that make branching hard in small lakes. First, the mean trait in the monomorphic resident drifts around  $u^*$  such that during extended periods selection is directional rather than disruptive. Second, incipient branches may go extinct soon after branching.

#### *Drift away from the evolutionary branching point*

The first process, movement of the monomorphic resident away from  $u^*$ , may be explained by either a direct or an indirect effect of demographic stochasticity: (i) random genetic drift,

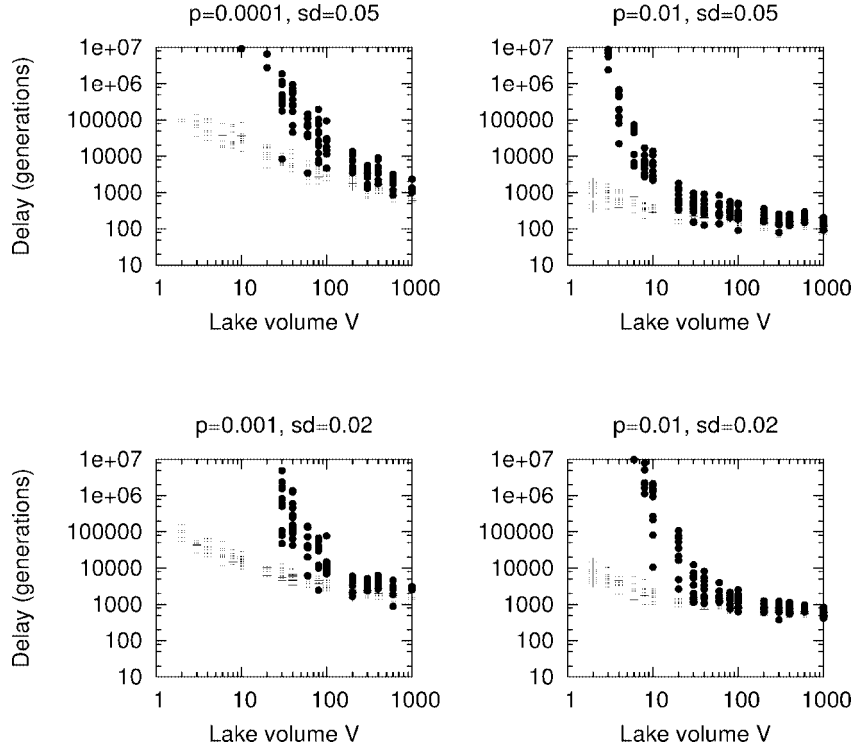


**Fig. 4.** Approach time  $t_A$  (plus symbols) and branching delay  $\Delta_B$  (solid circles) for four different combinations of  $P$  and  $\sigma$  and trade-off parameters based on Arctic charr (Fig. 1e–h). Time is expressed in units of the average life span ( $1/\mu$ ). All runs with  $V = 1$  are extinct before approaching the attractor. Parameters:  $K_1 = K_2 = 1$ ,  $\delta_1 = \delta_2 = 1$ ,  $\mu = 0.1$ .

in which case  $\hat{u}$  changes randomly and hence possibly against the fitness gradient; or (ii) the consequence of variation in the fitness gradient caused by random variation in the consumer population (in terms of abundance and trait distribution). In the former case, demographic stochasticity affects the trait distribution directly (e.g. by chance individuals on one end of the distribution reproduce more frequently or die less frequently than on the other side). In the latter case, the stochastic effect is indirect: random effects in the consumer population result in an imbalance of the two resources, creating a fitness gradient pointing away from the evolutionary singular point  $u^*$ . To distinguish between these two alternative explanations, we analyse a time series of the dynamics in a lake volume of  $V = 40$  and a symmetric trade-off. During an interval of 20,000 generations, the consumer population fluctuates steadily around  $n \approx 748$  ( $\tilde{n}$  for  $u = 0.5$ ) while the two resources display complementary trends in their densities (Fig. 5a, b). The trends in the resources are strongly correlated to fluctuations in the mean trait value,  $\hat{u}$  (Fig. 5d). The instantaneous fitness gradient is found by differentiating the per capita growth rate  $W = \beta(u) - \mu$  (cf. equation 4) with respect to  $u$ :

$$\frac{dW}{du} = F_1(t)(a_1 + 2b_1u) - F_2(t)(a_2 - b_2 + 2b_2u) \quad (7)$$

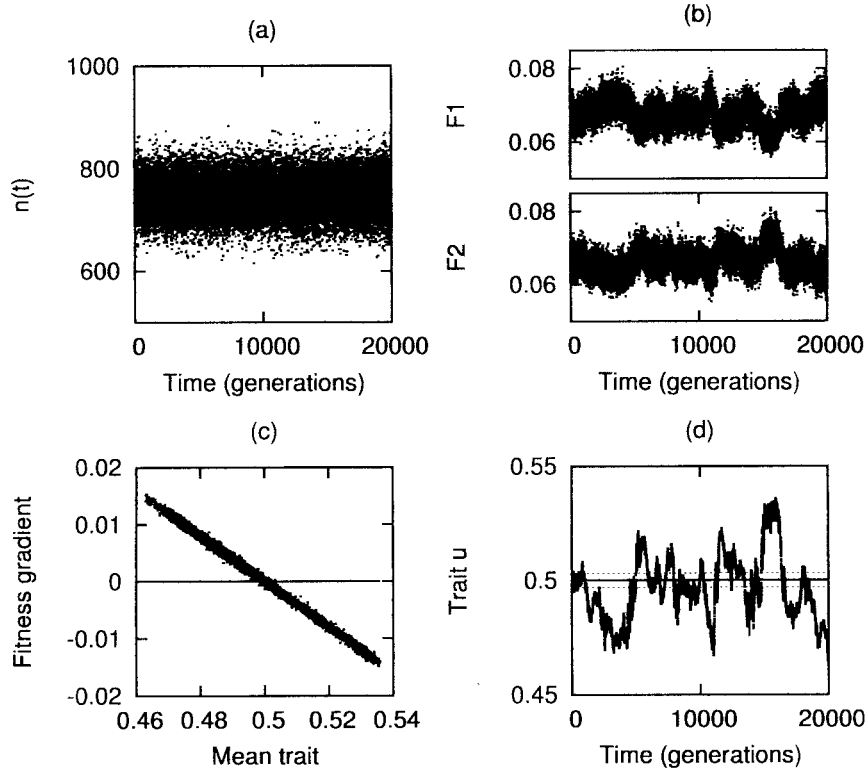


**Fig. 5.** A time series of the stochastic model in which no branching occurs, assuming a symmetric trade-off (Fig. 1a–d) and  $V = 40$ . (a) Consumer population abundance  $n(t)$ . (b) Food populations  $F_1(t)$  and  $F_2(t)$ . (c) Instantaneous fitness gradient (equation 7) vs. the mean trait in the population  $\hat{u}(t)$ . (d) The mean trait in the population  $\hat{u}(t)$ . The horizontal dotted lines indicate  $u = 0.497$  and  $u = 0.503$ , respectively (see text). Parameters:  $K_1 = K_2 = 1$ ,  $\delta_1 = \delta_2 = 1$ ,  $\mu = 0.1$ .

At regular intervals of 10 time units, the fitness gradient was plotted against the average trait in the population,  $\hat{u}$ . Figure 5c shows that only in a very narrow range around  $u^*$  ( $0.497 < \hat{u} < 0.503$ ) does the fitness gradient change sign due to random fluctuations. Yet Fig. 5d shows that  $\hat{u}$  moves away from  $u^*$  even outside this range (e.g. during the last 1500 generations). This implies that the mean trait moves against the fitness gradient during long periods, corresponding to the direct effect of demographic stochasticity (i.e. random genetic drift).

#### *Extinction of incipient branches*

The second process, extinction of incipient branches, may result from two causes: (i) drift-induced ‘forced’ extinction, or (ii) demographic ‘chance’ extinction. Random genetic drift could result in the pair of incipient species ( $\hat{u}_1$ ,  $\hat{u}_2$ ) moving out of the co-existence area (Fig. 1d), followed by the sure extinction of one of the two branches. To investigate this possible explanation, we analyse a number of extinction events in detail. Figure 6 shows the dynamics of two incipient branches in terms of their abundances,  $n_1(t)$  and  $n_2(t)$ , and their mean traits,  $\hat{u}_1(t)$  and  $\hat{u}_2(t)$ . According to our criterion for branching (see definition of  $t_B$ ,

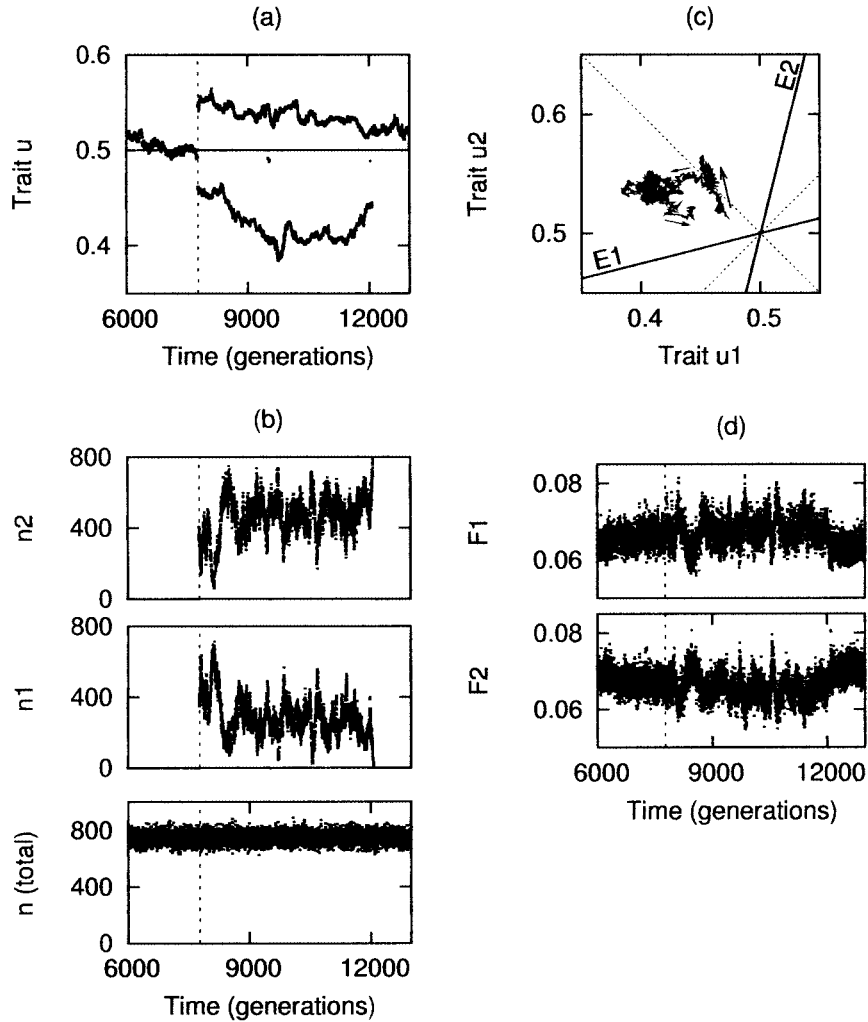


**Fig. 6.** Time series of the stochastic model: branching is followed by extinction of an incipient branch. Trade-off is symmetric (Fig. 1a–d) and  $V = 40$ . Vertical dashed lines indicate the moment of evolutionary branching at time  $t_B = 7800$  generations. (a) Mean trait in the two branches  $\hat{u}_1$  and  $\hat{u}_2$ . During the monomorphic phases, the mean trait  $\hat{u}$  is given. (b) Abundance of the two branches  $n_1$  and  $n_2$  and total abundance  $n_1 + n_2$ . (c) Trajectory of  $(\hat{u}_1, \hat{u}_2)$  in the trait evolution plot (TEP) (cf. Fig. 1d). Lines E1 and E2 are the extinction boundaries of  $n_1$  and  $n_2$ , respectively, and limit the co-existence area. Note that when  $n_1$  goes extinct,  $(\hat{u}_1, \hat{u}_2)$  is close to E1. (d) The food populations  $F_1(t)$  and  $F_2(t)$ . Parameters:  $K_1 = K_2 = 1$ ,  $\delta_1 = \delta_2 = 1$ ,  $\mu = 0.1$ .

p. 60), the population branches at  $t_B = 7800$  generations. At their origin, the two incipient branches have similar abundances ( $n_1(t_B) = 393$ ,  $n_2(t_B) = 349$ ). The numbers in the two branches, however, fluctuate considerably and these fluctuations are reflected in the resource densities (Fig. 6b, d). Figure 6c shows the trajectory of  $(\hat{u}_1, \hat{u}_2)$  in the trait evolution plot (cf. Fig. 1d). The expected path of  $(\hat{u}_1, \hat{u}_2)$ , based on the deterministic model, is along

the sub-diagonal from the EBP (0.5, 0.5) towards complete divergence (0, 1) (see arrow in Fig. 1d). Branch  $n_1$  goes extinct eventually; if this were a ‘forced’ extinction owing to random drift, then the actual trajectory of  $(\hat{u}_1, \hat{u}_2)$  should drift towards the extinction boundary of  $n_1$  (E1 in Fig. 6c). The plotted trajectory does indeed drift in this direction. The extinction of  $n_1$  may thus be the result of random drift of  $(\hat{u}_1, \hat{u}_2)$  reducing the expected abundance of this branch, although extinction occurs already before reaching the limit of the co-existence boundary.

To verify the generality of this observation, we analysed 33 simulations of 20,000 generations with parameters as in Fig. 6, in which 90 extinction events were recorded. We determined the trajectory of  $(\hat{u}_1, \hat{u}_2)$  prior to extinction. In 79% of cases, we found that the extinct branch was closer to its extinction boundary than the other branch (as in Fig. 6). This result suggests that the extinction events can be partly attributed to random drift. The 21% of cases, however, suggest that ‘chance’ extinction occurs as well.

With respect to ‘chance’ extinction, we note that during the initial phase of divergence  $\hat{u}_1$  and  $\hat{u}_2$  are so similar that the dynamics of  $n_1$  and  $n_2$  are almost neutral ( $n_1$  and  $n_2$  are interchangeable for  $u_1 = u_2$ ). In mathematical terms, if  $u_1 \approx u_2$  there is a stable equilibrium but its leading eigenvalue is almost zero such that fluctuations in  $n_1$  and  $n_2$  are not easily dampened. To check this idea we extended the deterministic model (equations 4–6) to two consumer populations  $N_1$  and  $N_2$ , and computed the eigenvalues of the equilibrium of the ecological dynamics, assuming symmetric divergence ( $u_2 = 1 - u_1$ ). The first eigenvalue  $\lambda_1 \approx 0$  for  $\hat{u}_1 \approx 0.5$  and decreases slowly as  $\hat{u}_1$  and  $\hat{u}_2$  diverge. This deterministic model predicts that, following a perturbation, the total consumer density  $N_1 + N_2$  converges quickly to its equilibrium value, while  $N_1$  and  $N_2$  converge very slowly to their respective steady states, mirrored by  $F_1$  and  $F_2$ . Analogously, in the IBM the large fluctuations of  $n_1$  and  $n_2$  are complementary such that  $n_1 + n_2$  remains more or less constant (Fig. 6b). The near-neutral stability ( $\lambda_1 \approx 0$ ) of the dimorphic equilibrium with small divergence ( $\hat{u}_1 \approx \hat{u}_2$ ) means that fluctuations of  $n_1$  and  $n_2$ , caused by demographic stochasticity, are not readily dampened. This permits large, long-term fluctuations, which may lead to extinction of one of the branches.

We postulate that incipient branches are sensitive to ‘chance’ extinction owing to the near-neutral stability of the dimorphic equilibrium. Drift, however, results in a bias in the extinction probability: the branch that is closest to its extinction boundary is most likely to go extinct.

## DISCUSSION

With a simple model we have shown that the absolute population size may influence the outcome of evolutionary dynamics. Only in large populations is evolutionary branching predicted to occur upon reaching the evolutionary branching point (EBP). In small populations, branching is predicted to be delayed. The delay increases quickly with decreasing absolute population size. Below a certain population size, the delay can be so long that on any relevant time scale (say, up to  $10^6$  generations) branching is not expected to occur at all. Based on this result, we expect that evolutionary branching has occurred more frequently in large than in small populations.

We identified two mechanisms that contribute to the delay in evolutionary branching. First, random genetic drift of the mean trait in the population causes the population to spend long periods (many consecutive generations) away from the EBP. During such time

intervals, selection is not disruptive but directional and branching is hence not expected to occur.

Second, soon after branching the incipient branches are prone to ‘chance’ extinction. The reason is that individuals of the two branches are almost substitutable because their trait values are very similar. The *relative* dynamics of the two branches are hence almost neutral: a perturbation in the ratio  $n_1/n_2$  is restored very slowly. The contrast in time scales between (slow) relative dynamics of similar phenotypes and (fast) aggregate dynamics of the total consumer density was recently analysed by Meszéna *et al.* (2005), who studied the dynamics of a number of similar clones in a (unimodal) distribution. Our result suggests that their result is relevant even for the dimorphic dynamics soon after branching. We hypothesize that the contrast between relative and aggregate dynamics explains the frequent extinction of incipient branches in small systems with demographic stochasticity. However, owing to random drift, the two branches do not have equal probability to go extinct. The one that is closest to its extinction boundary is most likely to disappear.

We have shown that quantitatively, these effects depend on the mutation rate and step size. In addition, they depend on the strength of directional and disruptive selection. Increasing the curvature of the trade-off (Fig. 1b) reduces the branching delay (especially in small lakes) and allows for branching in smaller lakes. The qualitative pattern, however, of the relation between  $V$  and  $\Delta_B$  remains the same (data not shown).

### The role of random genetic drift

Random genetic drift, resulting from ‘sampling error’ and finite population size, is one of the basic mechanisms of evolution, together with mutation and natural selection. Drift may decrease genetic variation or produce large shifts in allele frequencies (e.g. the founder effect) (Gavrilets, 2004). Allopatric speciation is usually seen as a by-product of divergence by random genetic drift (or by directional selection) in geographically isolated populations (Mayr, 1963; Provine, 2004). Yet in adaptive dynamics theory, the roles of drift and finite population size have received little attention (but see Proulx and Day, 2001; Cadet *et al.*, 2003; Parvinen *et al.*, 2003). In the recent polemic on adaptive dynamics and population genetics, it has been suggested that the effect of absolute population size on evolutionary dynamics can be scaled away by tuning the mutation rate (criticized by Waxman and Gavrilets, 2005b). Our results clearly falsify this assertion: the absolute population size *per se* may influence evolutionary dynamics through both drift and demographic extinction.

We found that random genetic drift can give rise to long delays of evolutionary branching. This means that random drift *demotes* speciation, a result that is in contrast with its role in classic allopatric speciation theory.

In small populations, random drift results in a weak coupling of changes of the genotype distribution and the fitness gradient. We found that the mean trait  $\hat{u}$  may move against the fitness gradient during long periods, spanning many generations. This observation has implications for the evolution of small populations and of exploited fish populations in particular. It has been argued that exploitation of fisheries stocks has caused a fast evolutionary response (Olsen *et al.*, 2004). However, most stocks are heavily depleted and hence at very low densities. This means that based on our results we do not expect genetic changes directed by the fitness gradient imposed by fisheries, but rather by random drift.

## ACKNOWLEDGEMENTS

We thank S. Legendre, N. Champagnat, A. Lambert, and J.A.J. Metz for discussions on the evolutionary branching in stochastic populations. Eva Kisdi and two anonymous reviewers provided thoughtful comments that helped to improve the manuscript. D.C. and A.M.dR. acknowledge financial support by the Dutch Science Foundation (NWO).

## REFERENCES

- Andersson, J. 2003. Effects of diet-induced resource polymorphism on performance in Arctic char (*Salvelinus alpinus*). *Evol. Ecol. Res.*, **5**: 213–228.
- Andersson, J., Johansson, F. and Söderlund, T. 2005. Interactions between predator- and diet-induced phenotypic changes in body shape of crucian carp. *Proc. R. Soc. Lond. B*, **273**: 431–437.
- Cadet, C., Ferrière, R., Metz, J.A.J. and van Baalen, M. 2003. The evolution of dispersal under demographic stochasticity. *Am. Nat.*, **162**: 427–441.
- Champagnat, N., Ferrière, R. and Ben Arous, G. 2001. The canonical equation of adaptive dynamics: a mathematical view. *Selection*, **2**: 73–83.
- Claessen, D. and Dieckmann, U. 2002. Ontogenetic niche shifts and evolutionary branching in size-structured populations. *Evol. Ecol. Res.*, **4**: 189–217.
- Day, T. 2000. Spatial heterogeneity and disruptive selection. *Am. Nat.*, **155**: 790–803.
- Day, T. and McPhail, J.D. 1996. The effect of behavioural and morphological plasticity on foraging efficiency in the threespine stickleback (*Gasterosteus* sp.). *Oecologia*, **108**: 380–388.
- Desharnais, R.A., Costantino, R.F., Cushing, J.M., Henson, S.M., Dennis, B. and King, A.A. 2006. Experimental support of the scaling rule for demographic stochasticity. *Ecol. Lett.*, **9**: 537–547.
- Dieckmann, U. and Doebeli, M. 1999. On the origin of species by sympatric speciation. *Nature*, **400**: 354–357.
- Dieckmann, U. and Law, R. 1996. The dynamical theory of coevolution: a derivation from stochastic ecological processes. *J. Math. Biol.*, **34**: 579–612.
- Gavrilets, S. 2004. *Fitness Landscapes and the Origin of Species*. Princeton, NJ: Princeton University Press.
- Geritz, S.A.H., Kisdi, É., Meszén, G. and Metz, J.A.J. 1998. Evolutionarily singular strategies and the adaptive growth and branching of the evolutionary tree. *Evol. Ecol.*, **12**: 35–57.
- Kisdi, É. and Geritz, S.A.H. 1999. Adaptive dynamics in allele space: evolution of genetic polymorphism by small mutations in a heterogeneous environment. *Evolution*, **55**: 993–1008.
- Kuznetsov, Y.A. 1995. *Elements of Applied Bifurcation Analysis*. Applied Mathematical Sciences Vol. 112. New York: Springer.
- Mayr, E. 1963. *Animal Species and Evolution*. Cambridge, MA: Harvard University Press.
- Meszén, G., Gyllenberg, M., Jacobs, F.J. and Metz, J.A.J. 2005. Link between population dynamics and dynamics of Darwinian evolution. *Phys. Rev. Lett.*, **95**: 078105.
- Metz, J.A.J., Nisbet, R.M. and Geritz, S.A.H. 1992. How should we define ‘fitness’ for general ecological scenarios? *Trends Ecol. Evol.*, **7**: 198–202.
- Metz, J.A.J., Geritz, S.A.H., Meszén, G., Jacobs, F.J.A. and van Heerwaarden, J.S. 1996. Adaptive dynamics: a geometrical study of the consequences of nearly faithful reproduction. In *Stochastic and Spatial Structures of Dynamical Systems* (S.J. van Strien and S.M.V. Lunel, eds.), pp. 183–231. Amsterdam: North-Holland.
- Olsen, E., Heino, M., Lilly, G., Morgan, M., Brattey, J., Ernande, B. *et al.* 2004. Maturation trends indicative of rapid evolution preceded the collapse of northern cod. *Nature*, **428**: 932–935.
- Parvinen, K., Dieckmann, U., Gyllenberg, M. and Metz, J.A.J. 2003. Evolution of dispersal in metapopulations with local density dependence and demographic stochasticity. *J. Evol. Biol.*, **16**: 143–153.

- Persson, L., Leonardsson, K., de Roos, M., Gyllenberg, M. and Christensen, B. 1998. Ontogenetic scaling of foraging rates and the dynamics of a size-structured consumer-resource model. *Theor. Pop. Biol.*, **54**: 270–293.
- Proulx, S.R. and Day, T. 2001. What can invasion analyses tell us about evolution under stochasticity in finite populations? *Selection*, **1–2**: 1–15.
- Provine, W. 2004. Speciation in historical perspective. In *Adaptive Speciation* (U. Dieckmann, M. Doebeli, J.A.J. Metz and D. Tautz, eds.), pp. 17–29. Cambridge: Cambridge University Press.
- Riley, J.G. 1979. Evolutionary equilibrium strategies. *J. Theor. Biol.*, **76**: 109–123.
- Robinson, B.W. and Wilson, D.S. 1995. Experimentally induced morphological diversity in Trinidadian guppies (*Poecilia reticulata*). *Copeia*, **2**: 294–305.
- Rueffler, C., Van Dooren, T. and Metz, J.A.J. 2004. Adaptive walks on changing landscapes: Levins' approach extended. *Theor. Pop. Biol.*, **65**: 165–178.
- Rueffler, C., Van Dooren, T.J.M. and Metz, J.A.J. 2006. The evolution of resource specialization through frequency-dependent and frequency-independent mechanisms. *Am. Nat.*, **167**: 81–93.
- Schaffer, M.E. 1988. Evolutionarily stable strategies for a finite population and a variable contest size. *J. Theor. Biol.*, **132**: 469–478.
- Schreiber, S.J. and Tobiasen, G.A. 2003. The evolution of resource use. *J. Math. Biol.*, **47**: 56–78.
- Van Dooren, T. 2005. The future of a mutation-limited toolbox. *J. Evol. Biol.*, **18**: 1158–1161.
- van Doorn, G., Dieckmann, U. and Weissing, F. 2004. Sympatric speciation by sexual selection: a critical re-evaluation. *Am. Nat.*, **163**: 709–725.
- van Tienderen, P.H. and de Jong, G. 1986. Sex ratio under the haystack model: polymorphism may occur. *J. Theor. Biol.*, **122**: 69–81.
- Waxman, D. and Gavrillets, S. 2005a. 20 questions on adaptive dynamics. *J. Evol. Biol.*, **18**: 1139–1154.
- Waxman, D. and Gavrillets, S. 2005b. Issues of terminology, gradient dynamics and the ease of sympatric speciation in adaptive dynamics. *J. Evol. Biol.*, **18**: 1214–1219.

## APPENDIX: DISCRETE EVENT SIMULATION

The simulation proceeds by stepping from one discrete event (birth or death) to the next. In between events, the model allows for resource dynamics. At time  $t$ , the timing of the next event to take place (be it a death or birth event) is determined from the total event rate,

$$E(t) = n(t)\mu + \sum_{i=1}^{n(t)} \beta(u_i)$$

where  $\beta(u_i)$  is the rate at which an individual with trait  $u_i$  gives birth (equation 1). Assuming the events are exponentially distributed, the timing of the next event is chosen as

$$t_{\text{next}}(t) = t + \frac{\ln(1+z)}{E(t)}$$

where  $z$  is a random number drawn from a uniform distribution. In between discrete events, the food populations change according to differential equations (equations 8–9) that are integrated with a simple Euler method (or assumed to be in quasi-steady state; see below). The integration step size  $\Delta t$  is either  $t_{\text{next}}(t) - t$  or  $\tau$ , whichever is smaller ( $\tau = 0.1$  by default). After each event and each integration step, the rates  $\beta(u_i)$  and  $E(t)$  and the event time  $t_{\text{next}}$  are updated to the current food densities. If the time of the next event is reached, an individual is chosen from the population randomly but weighed by the individuals' event

rates  $\mu + \beta(u_i)$ . With probability  $\beta(u_i)/(\beta(u_i) + \mu)$ , the chosen individual reproduces one offspring, otherwise it dies.

The ordinary differential equations for the dynamics of the food populations in the individual-based model are:

$$\frac{dF_1}{dt} = \delta_1(K_1 - F_1(t)) - F_1(t) \sum_{i=1}^{n(t)} \frac{A_1(u_i)u_i}{V} \quad (\text{A1})$$

$$\frac{dF_2}{dt} = \delta_2(K_2 - F_2(t)) - F_2(t) \sum_{i=1}^{n(t)} \frac{A_2(u_i)(1 - u_i)}{V} \quad (\text{A2})$$

Since resource dynamics are fast relative to consumer dynamics ( $\delta_i \gg \mu$ ),  $F_1(t)$  and  $F_2(t)$  can be assumed to be in steady state with the current consumer population. By setting  $dF_1/dt = 0$  and  $dF_2/dt = 0$ , we find the quasi-steady state resource levels:

$$\bar{F}_1(t) = \frac{K_1}{1 + \frac{1}{\delta_1 V} \sum_{i=1}^{n(t)} A_1(u_i)u_i} \quad (\text{A3})$$

$$\bar{F}_2(t) = \frac{K_2}{1 + \frac{1}{\delta_2 V} \sum_{i=1}^{n(t)} A_2(u_i)(1 - u_i)} \quad (\text{A4})$$

We use either equations (A1–A2) or equations (A3–A4); the results are indistinguishable.

